Progress In Electromagnetics Research C, Vol. 38, 241–257, 2013

IMPROVED METHOD OF NODE AND THRESHOLD SELECTION IN WAVELET PACKET TRANSFORM FOR UWB IMPULSE RADIO SIGNAL DENOISING

Abul K. M. Baki[1, *] and Nemai C. Karmakar[2]

[1]School of Engineering and Computer Science, Independent University, Bangladesh (IUB), Block # B, Basundhara R/A, Dhaka-1229, Bangladesh

[2]Department of Electrical & Computer Systems Engineering, Monash University, Building 72, Clayton, VIC 3800, Australia

Abstract—Ultra wide band (UWB) impulse radio (IR) technology has different applications in different sectors such as short range radios and collision avoidance radar. A strong signal denoising method is needed for UWB-IR signal detection. One of the challenges of UWB-IR signal detection technique is the environmental interferences and noises. Wavelet Packet Transform (WPT) based multi-resolution analysis technique is suitable for this kind of signal denoising and detection. The paper describes a better method of denoising and detection technique of UWB-IR signal based on calculation of energies of the coefficients of each WPT terminal-node and by using an improved threshold calculation technique. The proposed technique is investigated through both simulation and experimentation.

1. INTRODUCTION

Next generation wireless users will witness the use of Ultra Wide Band (UWB) impulse radio (IR) technology with the increased demand of bandwidth, power consumption and congestion of frequency spectrum. The journey of impulse radio technology dates back to 1880, with the experiment of German physicist Henrich Rudlof Hertz, and the radio frequency (RF) transmission experiment in 1901, conducted by Italian-born radio pioneer Guglielmo Marconi [1, 2]. The applications of UWB-IR technology are being observed in the field of collision avoidance vehicular radar, flow measurement, medical

Received 17 January 2013, Accepted 25 March 2013, Scheduled 8 April 2013

* Corresponding author: Abul Kalam Mohammed Baki (baki.akalam@gmail.com).

imaging, military communications, radar imaging, short range radios, surveillance, vibration measurement (non-contact) and many more. UWB-IR signals are very short duration pulses (sub-nano seconds) of very low duty cycle (on the order of 1/100 or 1/1000), low power spectral density and wide instantaneous bandwidth. According to Federal Communication Commission (FCC) the fractional bandwidth BW $[= (f_H - f_L)/f_C]$ of an IR signal should be $\geq 20\%$, or total BW $> 500\,\text{MHz}$. Here f_L and f_H are the lower $-10\,\text{dB}$ and higher $-10\,\text{dB}$ radiation points. The center frequency f_C can be found out from $(f_H + f_L)/2$. The short duration pulses of IR technology can be modeled by Gaussian type function [3, 4]. UWB-IR signal detection technique requires a very strong signal denoising technique because of the environmental interferences and noises. The noises and interferences may come from narrow band or wide band sources.

Wavelet Packet Transform (WPT), which has multi-resolution signal decomposition and synthesis property, can be used for IR signal denoising. By using this technique it is possible to decompose the noisy signal into various frequency sub-bands and later reconstruct it by choosing signals from some selected frequency bands. An improved denoising method of IR signal, based on energy calculation of the coefficients of the terminal nodes of WPT [4] and an improved threshold selection method, is proposed in this paper. Estimation of the energy content on each terminal node of WPT is a better approach than the estimation of energy of each level of discrete wavelet transform (DWT) for UWB-IR signal detection. DWT decomposes only approximate information into each successive level. On the other hand WPT decomposes both detailed and approximate information into each successive level which is helpful in detecting UWB signal.

This paper describes the denoising method of simulated and experimental UWB-IR signal. The experimental detection was performed in an anechoic chamber and in a noisy environment. The proposed WPT based denoising technique was applied to the received noisy signal. A 3×2 wide band smart antenna was used for the signal detection. The proposed signal denoising method can also be applied to ubiquitous health monitoring system and other wireless technology.

The paper is organized as follows. The model of UWB-IR signal and noises those can corrupt the detection system are discussed in Section 2. The concept of band selective smart antenna and its benefits are described in Section 3. Concept of WPT, improved method of node and mother wavelet selection is described in Section 4. An improved method of threshold selection technique is also described in Section 4. Experimental investigations of the proposed WPT based denoising technique is described in Section 5. Finally the conclusion is made

in Section 6.

2. UWB IMPULSE RADIO SIGNAL AND INTERFERENCES

2.1. Nature of Impulse Radio Signal

The frequency spectrum of UWB-IR depends on the rise-time of the pulse shape and falls within the frequency rang 650 MHz $\sim$ 5 GHz. It is mentioned in Section 1 that the duration of IR signal is within the sub-nano seconds and has a very wide instantaneous bandwidth. An impulse radio pulse can be modeled by using the following Gaussian function [4]:

$$y[i] = x_i A\sqrt{e}2\pi f_c e^{-2(x_i \pi f_c)^2} \tag{1}$$

A Gaussian modulated impulse radio signal can be represented by:

$$y_m[i] = Ae^{-m(i*\Delta t-d)^2}\cos[2\pi f_c\,(i*\Delta t-d)] \tag{2}$$

In (1) and (2),

$x_i = i \times (\Delta t - d), \quad i = 0, 1, \ldots, N-1;$
$N =$ number of samples;
$A =$ amplitude;
$d =$ delay;
$f_c =$ center frequency (Hz);
$\Delta t =$ sampling interval;
$w =$ normalized bandwidth;

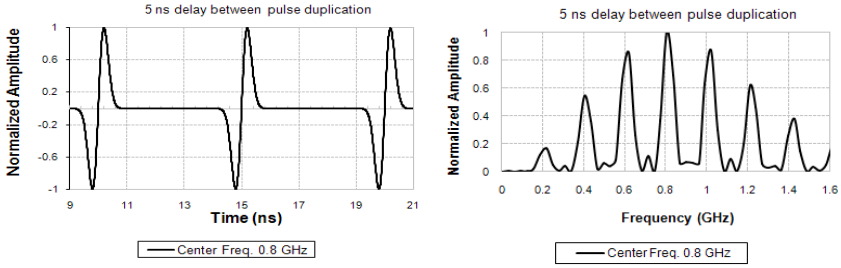

(a) (b)

Figure 1. (a) Impulse radio pulses of centre frequency 800 MHz. (b) Power spectrum of the pulse trains of Figure 1(a).

b = attenuation;
$m = \frac{5\pi^2 w^2 f_c^2}{b * \ln(10)}$.

Though IR signal is wideband in nature, most of the energy of a particular type of pulse is concentrated on or around a particular frequency or narrow frequency bands. Figure 1(a) shows the time-domain and Figure 1(b) shows the frequency-domain natures of IR pulses of centre frequency 800 MHz. It can be seen from Figure 1(b) that the energy contents of the pulse train are mainly concentrated at and around its center frequency.

2.2. Interferences and Noises in Impulse Radio Signal Detection

It was mentioned in Section 1 that the main sources of noises and interferences in IR signal detection can come from narrow band or wide band signals. They may come from narrow band communication channels, mobile phones, TV broadcastings, background white noises, corona in air, vehicles generated interferences and other wireless networks.

The following types of interferences and noises can corrupt an impulse radio signal:

i. Discrete spectral interferences from amplitude and frequency modulated narrow band signals.
ii. Wideband repetitive pulses from other sources.
iii. Wideband random pulses from lightning or RF corona, or car ignition.
iv. Wideband white and stochastic noises and ambient noises.

3. WIDE BAND ANTENNA FOR IMPULSE RADIO SIGNAL DETECTION

It has been experimentally verified that the maximum transmission/reception can further be improved by adjusting the weighting functions of the array elements [5, 6] of smart antenna [7, 8]. The concepts of smart antenna are discussed in details in [9, 10]. A band selective smart antenna with gain enhancement and wavelet based signal processing capabilities can cancel the interferences and noises and enhances the effective SNR of the desired IR signal. The property of the band selective smart antenna will reduce the effect of noises and interferences and enhance the strength of the received signals. A 3×2 element prototype smart antenna [9] was used to capture the IR signal.

The measured return loss of a single element is shown and discussed in [9]. The pulse-like interferences may have characteristics very similar to IR signals and may have amplitude much larger than that of IR signal. The selection of quiet band for signal detection through a smart antenna and a WPT based method will enhance the separation of other pulse-like and narrowband interferences from the signal. The property of the used smart antenna will reduce the effect of noises and interferences those are out of the frequency band of the antenna and enhance the strength of the signal received within the frequency band. It will be discussed later that the band of operation of the antenna plays a significant role in selecting the mother wavelet for WPT.

4. WAVELET PACKET TRANSFORM

4.1. Theory of Wavelet Packet Transform

WPT decomposes the original signal into approximate (lower frequency part) and detailed (higher frequency part) components using complementary filters [11] in each successive level. In WPT, it is possible to have the signals' statistical information (e.g., standard deviation, mean, cumulative energy etc.) from each of the terminal nodes. Thus WPT predicts the noise and signal dominant nodes. In real situations noise will dominate in some of the nodes and in other nodes desired signal will dominate. After analyzing the statistical information of each terminal node, nodes with dominant noise can be avoided during signal reconstruction. Threshold parameters can be applied to the coefficients of the selected nodes to enhance the SNR further. The noise dominant nodes can be detected and blocked by scanning the environment before signal detection. A particular node in WPT represents a set of coefficients which corresponds to a certain frequency band. Calculation process of WPT coefficients are described in [12, 13]. The output coefficients of node $(i,\, j)$ are obtained from the output coefficients of its parent node $(i-1,\, j/2)$ and generally can be expressed as [4, 14]:

$$w(n)_{i,j} = \sum_{k=0}^{L-1} h(k)_{j\%2} w\left(n - 2^{i-1}k\right)_{i-1,\frac{j}{2}} \tag{3}$$

where,

i is the number of level $(0 < i < J)$;

J is the number of maximum decomposition level;

j is the frequency band $(0 \le j < 2^i)$;

$n = 2il$, l is natural number, and

$w_{0,0}$ are the input samples.

Symbol '%' represents modulus operation.

Figure 2 shows an example block diagram of WPT decomposition tree up to decomposition level 3. In the block diagram 000, 001, 010, etc. represent the paths of the nodes. For example, 101 means that the signal is first passed through the high pass filter (HPF), and then through low pass filter (LPF), after that again through HPF. On the other hand, only paths 000 and 001 are available on the resolution level 3 of the Discrete wavelet Transform (DWT) since it decomposes only approximate information into each successive level. As a result, it is not possible to have signal information from node 010 up to node 111 in DWT denoising technique. H_0 (ω) and H_1 (ω) in Figure 2 are the frequency responses of LPF and HPF, respectively.

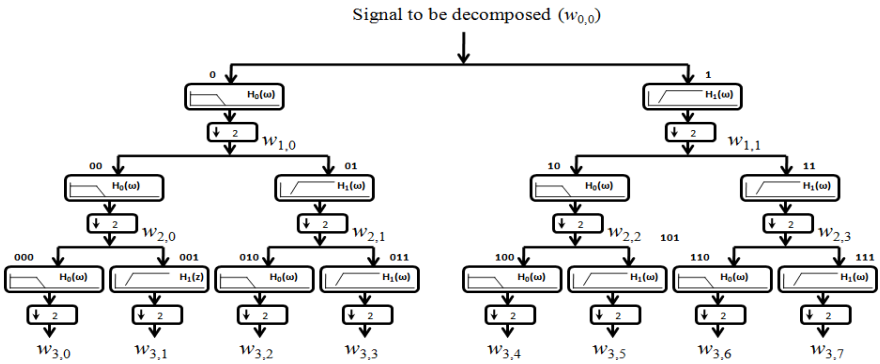

Figure 2. Block diagram of level-3 binary tree decomposition of wavelet packet transform (WPT).

4.2. Selecting an Optimal WPT Decomposition Tree

Most of the energy of a particular IR signal concentrates in a few nodes of different decomposition level of WPT. The nodes (those correspond to certain frequency bands) can be obtained by searching the optimal decomposition tree of WPT. An optimal decomposition tree can be searched with less number of nodes by using Shannon entropy criterion. Shannon entropy searches for an optimum decomposition tree based on the minimum entropy criterion, which is the smallest of the total entropy of all terminal nodes at a certain level in all the possible tree structures of WPT. Shannon entropy keeps the signal dominant nodes and removes the undesired or noise dominant nodes. Shannon entropy

(E_{sh}) was calculated by using (4):

$$E_{sh} = \sum_{i=1}^{n} \left[\left| w(n)_{i,j} \right|^2 \log \left[\left| w(n)_{i,j} \right|^2 \right] \right] \tag{4}$$

The calculated entropy of the WPT node coefficients varies over different scales dependent on the characteristics of the signals under investigation. Example of searching the optimal decomposition tree will be discussed in Section 4.3. Energy content of the node coefficients can be calculated [4] by using (5):

$$E_{i,j} = \sum_{k=1}^{n} \left| w(n)_{i,j} \right|^2 \frac{1}{\Omega} \tag{5}$$

where,

$w(n)_{i,j}$ = coefficients of node (i, j) and can be found by using (3);

$E_{i,j}$ is the energy content of node j of level i;

Ω is the impedance of the receiving system (normally 50 Ω);

Variance (σ^2) of the node coefficients can be calculated by using (6):

$$\sigma^2 = \frac{\sum (w(n)_{i,j} - \bar{c})^2}{n-1} \tag{6}$$

where $\bar{c}$ is the mean of the coefficients $w(n)_{i,j}$.

In (6), each time the mean of the coefficients is needed to be calculated for a new set of coefficients or samples which is not computationally efficient. Higher memory space is also required for the calculation of variance. Calculation of energy, based on (5), is easier and faster than the calculation of variance. Therefore calculation of energy contents of the node coefficients is a better approach.

4.3. Searching an Optimal Mother Wavelet

Though it is difficult to choose a mother wavelet for a particular noisy signal, an optimal mother wavelet was investigated that better suits an IR signal. Optimal mother wavelet can be determined from the characteristics of pulse shape. One factor for the selection of an optimal mother wavelet is the frequency bandwidth of the used antenna [15]. In the proposed IR signal detection technique, the bandwidth characteristic of the smart antenna will play a major role in optimal wavelet selection [4]. Following are the two parameters considered for optimal mother wavelet selection:

(i) The ratio of the energies of the selected nodes to those of total nodes.

(ii) Mean Squared Error (MSE) between the reconstructed and original signals.

The energy ratio is mainly dependent on the energy concentration of a particular signal and frequency bands of the selected nodes. Two different signals, IR signal-1 and IR signal-2, were considered in the investigation. Figures 3(a) and 4(a) show the noisy IR signal-1 and IR signal-2 respectively. Figure 3(b) shows the original as well as the denoised IR signal-1. Similarly Figure 4(b) shows the original as well as the denoised IR signal-2. Signal-1 was generated by using Gaussian modulated sine wave equation. Signal-2 was generated by using Gaussian mono pulse equation. The center frequencies of signal-1 and signal-2 were chosen respectively as 950 MHz and 500 MHz.

The noisy radio signals were fed separately to the input of WPT decomposition algorithm developed by using LabVIEW. The signals

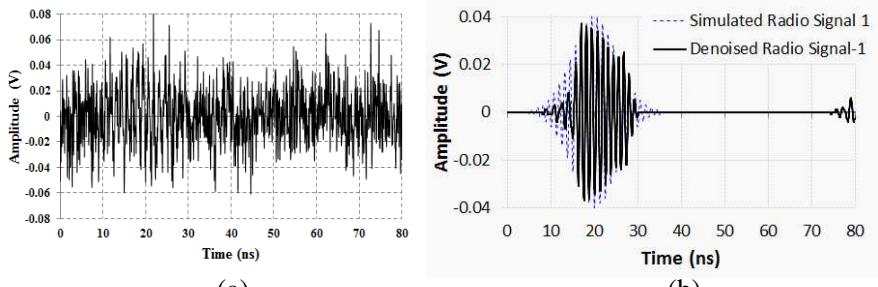

Figure 3. (a) IR signal-1 buried under noise. (b) Original and denoised IR signal-1.

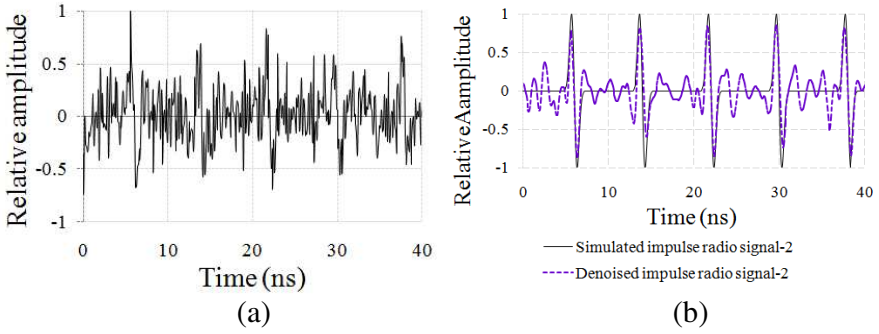

Figure 4. (a) IR signal-2 buried under noise. (b) Original and denoised IR signal-2.

were then reconstructed by taking the coefficients of the selected nodes (nodes with maximum energy contents) of the decomposition tree. Energy contents of IR signal-1 for all 32 nodes of decomposition level 5 are shown in Figure 5. Figure 5 shows that most of the energies are passing through nodes (5, 2) and (5, 6). These two nodes were selected for the reconstruction of IR signal-1. The ratio of the energies of the selected nodes to those of total nodes and the MSE were calculated for different Daubechies mother wavelets. The calculated normalized values are shown in Figure 6. Daubechies mother wavelets were chosen, since it was found that they show better performance than any other wavelets for these signals. Calculation method of MSE is discussed in [16]. Figure 6 shows that the maximum energy ratio and minimum MSE in the simulation are achieved for mother wavelets db 6 $\sim$ db 11. The sampling frequency, number of samples and WPT decomposition level were respectively 12.5 GHz, 1024 and 5 for both the signals. Figures 5 and 6 also show the experimental data of a signal, similar to IR signal-1, which will be discussed later in Section 5.

In Figure 5 energy contents of all the 32 nodes' coefficients are shown, which is computationally inefficient. Instead an optimal decomposition tree can be searched to achieve the same performance but with less number of nodes by using (4). One such optimal WPT decomposition tree for IR signal-1, based on the Shannon entropy, is shown in Figure 7. In Figure 7, first indices in the braces indicate the decomposition level i and the second indices indicate the number of node j of level i. Figure 7 shows that the energies of only the terminal nodes are needed to be compared instead of calculating those for all

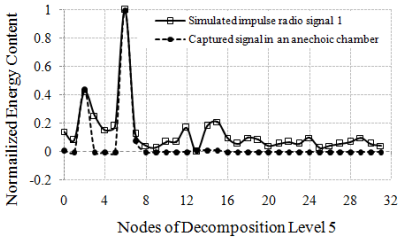

Figure 5. Energy contents of each node of WPT decomposition level 5 for simulated IR signal-1 and captured IR signal-1 in an anechoic chamber.

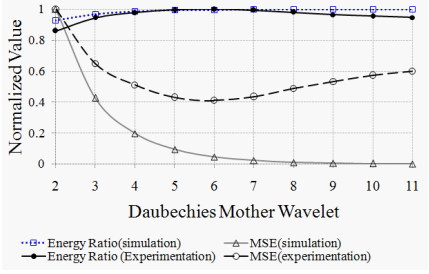

Figure 6. Normalized energy ratio and mean square error (MSE) for the simulated and experimental noisy IR signal-1 and for different Daubechies wavelets.

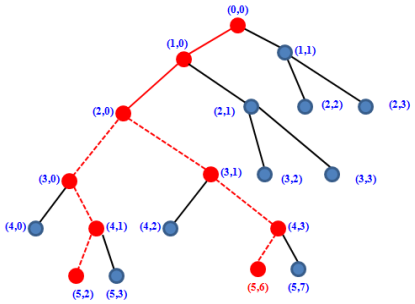

Figure 7. Optimal tree calculation for IR signal-1 by using Shannon entropy criteria. Most of the IR signal-1 passes through nodes (5, 2) and (5, 6).

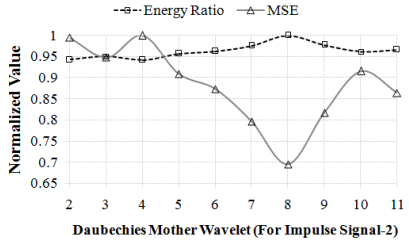

Figure 8. Normalized energy ratio and mean square error (MSE) for the reconstructed IR signal-2 and for different Daubechies mother wavelets.

the 32 nodes of level 5 (as shown in Figure 5). Similar simulated comparisons, as those have been described above, were also done for IR signal-2. The calculated Energy ratio and MSE for different mother wavelets are shown in Figure 8. In this case mother wavelet db 8 gave the optimum performance among the compared wavelets. Therefore mother wavelet db 8 was selected for further analysis of IR signal-2.

In some applications, such as atmospheric and oceanic datasets, the power spectra of wavelet transformation are found to be biased or distorted in favor of large scales or low frequencies; though some wavelet applications do not have this bias issue [17]. The frequency is narrower at larger scales of DWT and the peaks are sharper and may have higher amplitude. The biasing phenomenon was not observed across the optimal tree of the WPT nodes described above. Since WPT has the same frequency bandwidths in each resolution which is particularly suitable for non-stationary signals, it provides better resolution regardless of high or low frequencies [18].

4.4. Improved Method of Threshold Selection

One of the major steps of denoising is the estimation of WPT coefficients through threshold value selection. There are several threshold selection techniques. In Universal threshold selection rule, the threshold is:

$$\text{Thrsh} = \bar{\sigma}\sqrt{2 \cdot \log(n)} \tag{7}$$

where n is the total number of samples in the signal, and $\bar{\sigma}$ is the noise level estimated from the median filtering of the first detailed coefficients

and can be expressed [12] as:

$$\bar{\sigma} = \text{MAD}\left(c_{d\_1}\right)/0.6745 \tag{8}$$

$\text{MAD}(c_{d\_1})$ is the median absolute deviation of detailed coefficients of level 1.

The rescaling factor 0.6745, used in (8), makes the equation well suited for zero mean Gaussian white noise model [19]. It is mentioned earlier that, in (7) the standard deviation of noise level is estimated from the detailed coefficients of level 1. Another method of automatic threshold selection rule for wavelet denoising, based on the level dependent median value and number of coefficients, is described in [16]. The denoising method proposed in this paper uses a few terminal nodes of WPT. As a result, only the noises and interferences of the terminal nodes are needed to be considered and (7) can be modified as:

$$\text{Thrsh} = \bar{\sigma}_t \sqrt{2 \cdot \log(n_t)} \tag{9}$$

where, n_t is the number of coefficients of the terminal nodes, and

$$\bar{\sigma}_t = \text{MAD}_t/0.6745 \tag{10}$$

where, MAD_t is the median absolute deviation of the coefficients of the terminal nodes with only noises and interferences.

It was mentioned in Section 4.3 that Figures 3(a) and 4(a) show respectively the simulated noisy IR signal-1 and IR signal-2. The proposed threshold technique was applied to these noisy signals. Figures 3(b) and 4(b) show the denoised IR signals along with the original noise-free IR signals. The denoised signals were obtained from the noisy signals by applying the methods described in Sections 4.2 $\sim$ 4.3 and the threshold selection technique described earlier in this section. The average input SNR of the IR signal-1 was -8.87 dB and that of IR signal-2 was -5 dB. In each case, total 100 simulations were run. After denoising, average increase of SNR for IR signal-1 was 4.86 dB and that of IR signal-2 was 9 dB. The calculation process of the SNR is described in [4]. Figures 3 and 4 show that the proposed WPT based denoising method successfully recovered the IR signals from the corrupted ones. In real situations, noises and interferences of an environment, which will be discussed in Section 5, can be estimated before the signal detection.

5. EXPERIMENTAL RESULTS ON IMPULSE RADIO SIGNAL

Experimentations on IR signals were conducted by using an impulse signal generator, which can generate signal at 1 GHz. The rise time

and fall time of the signal source was 300 picoseconds and 100 ns respectively. Impulsive signals from the signal generator were captured by a 3×2 phased array antenna both inside and outside of an anechoic chamber. Since the intensity of the radiated signal is very low, it is difficult to capture this kind of signal with conventional antennas. A dipole antenna was used as a transmitting antenna. A digital oscilloscope of 50 GHz sampling frequency was connected with the 3×2 element antenna for signal detection. The sampling frequency of the captured signal was 6.25 GHz and the sample length was 5000. Energy contents of the captured signal for all 32 nodes of decomposition level 5 are shown in Figure 5 along with the simulated data. Experimental data of Figure 5 shows that most of the captured signal is also passing through nodes (5, 2) and (5, 6) of WPT tree. It has already been mentioned that most of the simulated IR signal-1 passes through nodes (5, 2) and (5, 6). Daubechies wavelet db 6 gave the optimum performance for the experimental data (Figure 6). Therefore Daubechies wavelet 6 (db 6) was selected for the reconstruction of this signal based on simulation and experimental investigations. DWT based denoising methods were also investigated but the performance of the method was not better. The reasons are explained hereafter. In DWT based methods, it is not possible to capture signals from both nodes (5, 2) and (5, 6). If DWT have had applied to this signal then it would have been possible to get these signals (along with some noises and interferences) from nodes (3, 0) and (3, 1) of Figure 7. Figures 5 and 7 show that the maximum signal energy is passing through WPT node (5, 6). But in case of DWT, nodes (3, 0) and (3, 1) include the noises and interferences of nodes (4, 0), (4, 2), (5, 3) and (5, 7) of WPT tree. In the proposed WPT based method, it is possible to block these noise dominant nodes.

During the experiment, environmental interferences and noises were captured before capturing the signal. Some signals from other communication channels were visible at 891, 952, 1820 and 2149 MHz frequencies. Later the captured noises and interferences were fed to the input of the WPT algorithm and the signals were reconstructed by taking only the coefficients from nodes (5, 2) and (5, 6). At this stage no threshold value was applied to the coefficients of these two nodes during the reconstruction in order to find out the natures of noises and interferences through these two nodes. Figure 9 shows the time-frequency (TF) plot of the reconstructed noises and interferences where the interferences of 891 and 952 MHz frequencies along with some noises exist. Since these interferences and noises fall within the bandwidth of the captured IR signal-1, it is necessary to cancel out the effect of these disturbances from these two nodes. It will be

shown later in this section that these kinds of in band interferences and noises can be reduced by applying the threshold technique discussed in Section 4.4. Next, the IR signal-1 was captured in the same noisy environment. Some simulated noise was further added to the captured signal to investigate the effectiveness of the developed denoising algorithm, particularly when the signal of interest is buried under noises. Figure 10 shows the captured signal along with the added noises. The SNR of this signal with artificially added noise was -7.24 dB.

Appropriate Daubechies mother wavelet was again sought for this noisy signal and the signal was reconstructed by taking the coefficients of terminal nodes (5, 2) and (5, 6) of the optimal WPT tree. The threshold technique described in Section 4.4 was applied to the selected coefficients of the two mentioned nodes during reconstruction of the signal. Figure 11 shows the TF plot of the reconstructed signal which shows that the proposed WPT algorithm can successfully recover a UWB-IR signal which is buried under in band noises and interferences. Figure 12 shows the time domain plots of originally captured IR signal-1 (in the anechoic chamber) and the denoised IR signal-1.

The comparison of the simulated and experimental results (Figure 6) strongly supports that the selection of an optimal wavelet (in this case db 6) is dependent on the nature of the signal and the frequency bandwidth of the receiving antenna. The TF plots shown in the paper are constructed by using Short Time Fourier Transform (STFT). It is noteworthy to mention here that the TF plots shown in this paper are only for the representation and comparison purposes. The proposed WPT based multi-resolution analysis technique is stronger than any other kind of fixed-resolution TF distribution.

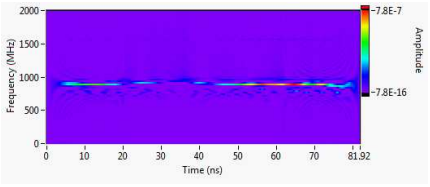

Figure 9. Time-frequency plot of reconstructed interferences and noises passing through nodes (5, 2) and (5, 6) of the WPT decomposition tree.

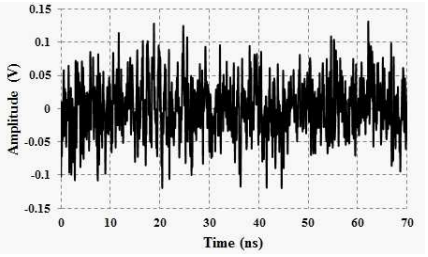

Figure 10. Captured IR signal-1 corrupted with environmental and artificially added noises and interferences.

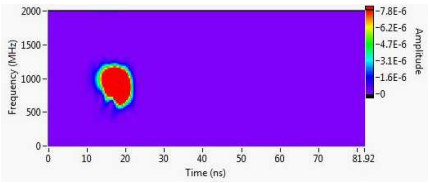

Figure 11. Time frequency (TF) plot of denoised IR signal-1.

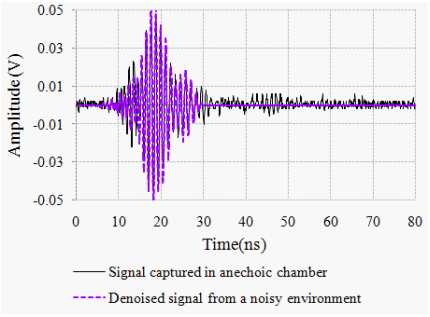

Figure 12. Initially captured IR signal-1 in an anechoic chamber and denoised signal from a noisy environment.

Therefore it is sufficient to implement only WPT based denoising technique without adding STFT method.

6. CONCLUSION

The detection of an ultra wide band (UWB) impulse radio (IR) signal from a noisy environment is a difficult task, particularly when the signal is buried under noises and interferences. An improved method of WPT nodes selection, based on calculation of the energy contents of the nodes' coefficients, is proposed in the paper. Energy-analysis based WPT denoising of IR signal is better than the variance based method of DWT. The DWT method decomposes only the approximate information which is not a better approach for UWB signals. An improved method of threshold selection technique is also investigated and proposed in the paper. Most of the energies of a particular IR signal are concentrated in a few terminal nodes of WPT. Different mother wavelets were compared to find out an optimal mother wavelet. The search for an optimal mother wavelet for a particular type of IR signal was done based on the energy ratios of the nodes and the MSE. The used wideband receiving antenna has the band selective, and gain enhancement capabilities. This kind of antenna is helpful for capturing the IR signal of certain frequency bands that reduces the noises and interferences of other frequency bands. The frequency band of the used antenna also played a major role in optimal wavelet selection. Experimentations on IR signals were performed in an anechoic chamber and in a noisy environment. The simulated IR signal-1 and the experimental IR signal-1 were identical. It is shown

in this paper through simulation, measurement and analysis that the proposed WPT based denoising method is an efficient tool for UWB-IR signal denoising and detection. The proposed WPT based detection system can successfully detect the impulse signal which is buried under noises. The method can also remove or reduce the effect of interferences and noises those fall within the same frequency band as that of an IR signal.

ACKNOWLEDGMENT

This work is supported by the Australian Research Council (ARC) Linkage Project Grant LP0989355. The authors also acknowledge the two anonymous reviewers for their careful reading and constructive comments.

REFERENCES

1. Guimaraes, D. A. and G. G. R. Gomes, "Introduction to ultra wideband radio," *Revista Telecomunicacoes*, Vol. 14, No. 01, 49–61, 2012.
2. Siwiak, K. and L. L. Huckabee, "Ultra wideband radio," *Wiley Encyclopedia of Telecommunications*, (J. G. Proakis, ed.), Vol. 5, 2754–2762, John Wiley & Sons, Inc., Hoboken, New Jersey, USA, 2003.
3. Hussain, M. G. M., "Principles of space-time array processing for ultra wide-band impulse radar and radio communications," *IEEE Transactions on Vehicular Technology*, Vol. 51, No. 3, 393–403, 2002.
4. Karmakar, N. C. and A. K. M. Baki, "Detection of UHF band impulse radio signal through wavelet packet transform," *7th International Conference on Electrical and Computer Engineering*, 867–871, Dhaka, Bangladesh, 2012.
5. Baki, A. K. M., N. Shinohara, H. Matsumoto, K. Hashimoto, and T. Mitani, "Study of isosceles trapezoidal edge tapered phased array antenna for solar power station/satellite," *IEICE Trans. Commun.*, Vol. E90-B, No. 4, 968–977, 2007.
6. Baki, A. K. M., K. Hashimoto, N. Shinohara, T. Mitani, and H. Matsumoto, "Isosceles-trapezoidal-distribution edge tapered array antenna with unequal element spacing for solar power satellite," *IEICE Trans. Commun.*, Vol. E91-B, No. 2, 527–535, 2008.

7. Baki, A. K. M., N. C. Karmakar, U. Bandara, and E. M. Amin, "Beam forming algorithm with different power distribution for RFID reader," *Chipless and Conventional Radio Frequency Identification: Systems for Ubiquitous Tagging*, 64–95, IGI Global, USA, May 2012, ISBN 978-1-4666-1616-5 (hardcover).
8. Baki, A. K. M. and N. C. Karmakar, "Staircase power distribution of array antenna for UHF band RFID reader," *7th International Conference on Electrical and Computer Engineering*, 854–857, Dhaka, Bangladesh, 2012.
9. Karmakar, N. C., P. Zakavi, and M. Kumbukage, "FPGA-controlled phased array antenna development for UHF RFID reader," *Handbook of Smart Antennas for RFID Systems*, 211–241, John Wiley & Sons, Inc., 2010.
10. Karmakar, N. C., "Recent paradigm shift in RFID and smart antenna," *Handbook of Smart Antennas for RFID Systems*, 57–82, John Wiley & Sons, Inc., 2010.
11. Naderi, M. S., G. B. Gharehpetian, and M. Abedi, "Modeling and detection of transformer internal incipient fault during impulse test," *IEEE Transactions on Dielectrics and Electrical Insulation*, Vol. 15, No. 1, 284–291, 2008.
12. Ruch, D. K. and P. J. Van Fleet, *Wavelet Theory an Elementary Approach with Applications*, John Wiley & Sons, Inc., 2009.
13. Atto, A. M., D. Pastor, and A. Isar, "On the statistical decorrelation of the wavelet packet coefficients of a band-limited wide-sense stationary random process," *Signal Processing*, Vol. 87, 2320–2335, 2007, online resource at www.sciencedirect.com.
14. Trenas, M. A., J. Lopez, and E. L. Zapata, "FPGA implementation of wavelet packet transform with reconfigurable tree structure," *Proceedings of the 26th Euro Micro Conference*, Vol. 1, 244–251, 2000.
15. Kawada, M., A. Tungkanawanich, and Z.-I. Kawasaki, "Detection of wide-band E-M signals emitted from partial discharge occurring in GIS using wavelet transform," *IEEE Trans. on Power Delivery*, Vol. 15, No. 2, 467–471, Apr. 2000.
16. Zhou, X., C. Zhou, and I. J. Kemp, "An improved methodology for application of wavelet transform to partial discharge measurement denoising," *IEEE Transactions on Dielectrics and Electrical Insulation*, Vol. 12, 586–594, 2005.
17. Liu, Y., X. S. Liang, and R. H.. Weisberg, "Rectification of the bias in the wavelet power spectrum," *J. Atmos. Oceanic Technol.*, Vol. 24, 2093–2102, 2007.

18. Xu, Y.-J. and S.-D. Xiu, "A new and effective method of bearing fault diagnosis using wavelet packet transform combined with support vector machine," *Journal of Computers*, Vol. 6, No. 11, 2502–2509, 2011.
19. Zhang, H., T. R. Blackburn, B. T. Phung, and D. Sen, "A novel wavelet transform technique for on-line partial discharge measurements. Part 1: WT denoising algorithm," *IEEE Transactions on Dielectrics and Electrical Insulation*, Vol. 14, No. 1, 3–14, 2007.